Desalination and Water Treatment
www.deswater.com

doi: 10.5004/dwt.2022.28454

262 (2022) 60–73
June

An eco-friendly hybrid sonophotocatalytic approach to optimize carpet washing wastewater treatment

Gamze Dogdu

Department of Environmental Engineering, Faculty of Engineering, Bolu Abant Izzet Baysal University, Golkoy Campus 14030, Bolu, Turkey, Tel. +90 (374)2541000(4905); email: gamzedogdu@ibu.edu.tr

Received 20 December 2021; Accepted 30 March 2022

ABSTRACT

The fundamental objective of this work is to examine the efficiency of the hybrid advanced treatment process for removal of residual organic pollutants in carpet washing wastewater at various reaction conditions. For this goal, Taguchi method was adopted to optimize the critical factors viz. catalyst type (TiO_2 and ZnO), catalyst concentration (0.5–2.5 g/L), pH (2–10), H_2O_2 concentration (0–10 mM), and operation time (30–180 min). These experimental factors were handled in mixed levels ($2^1 \times 3^4$), and operation parameters were optimized by the application of L_{18} tests. The analysis of variance results showed that catalyst type, H_2O_2 concentration, and pH had the highest effects on the elimination of chemical oxygen demand (COD) and color. COD and color removal efficiencies were determined as 53% and 99%, which are close to the predicted values of 49% and 95%, respectively, according to the confirmation test carried out under optimal parameters. Thus, considering the cost of energy consumed and acceptably high COD and color removal level, the sonophotocatalysis process combining ultrasound, ultraviolet, hydrogen peroxide, and catalyst (TiO_2 and ZnO) could achieve great performance for the reduction of pollution load in wastewater by the fast and eco-friendly removal of organic pollutants from carpet washing effluents.

Keywords: Carpet washing wastewater; Hybrid process; Sonophotocatalysis; Advanced oxidation; Taguchi design

1. Introduction

Carpets, comprising a portion of the textile industry, are used in small and large sizes, especially in homes, hotels, and other accommodation areas. Carpet washing (CW) is extensively practiced in homes and commercial premises to prolong the life of carpets and to ensure that living and working areas are hygienic. Especially in Asian countries such as Turkey, intensive carpet washing activity occurs in metropolitan and rural areas in the spring. The CW sector is known to consume substantial amounts of fresh water, along with other washing industries such as car washing and laundry. CW processes contain various hazardous pollutants, such as synthetic and organic chemicals; surfactants (including detergents and deodorizing products), dye residues, color, turbidity, suspended solids, chemical oxygen demand (COD), and other potentially hazardous, non-biodegradable chemicals and extracted carpet residues [1,2]. Therefore, if this wastewater is not correctly handled and treated, some carpet washing chemicals may damage the ecosystem, be toxic to aquatic life, and promote excessive algal growth due to their higher nutrient contents [3,4]. In addition to disruption of ecological balance, this type of water contributes to the rapid decrease in

1944-3994/1944-3986 © 2022 Desalination Publications. All rights reserved.

dissolved oxygen levels, as it has relatively low oxygen levels compared to real industrial wastewater. Hence, treatment and then reuse, or incorporating the wastewater into the infrastructure network system, may reduce the burden of the enterprise and urban treatment plants [5].

Advanced oxidation processes (AOPs) are extremely novel methods that have attracted more attention in the removal of the toxic recalcitrant and/or non-biodegradable organic and inorganic components present in wastewater that are resistant to conventional treatment methods [6,7]. In this context, some AOPs, including heterogeneous and homogeneous photocatalysis, sonolysis, Fenton, electro-Fenton, electrochemical, and ozonation reactions have shown considerable promise for wastewater treatment applications [8–13]. Among those processes, heterogeneous photocatalytic processes (HPC) are defined as the degradation of recalcitrant compounds in water/wastewater systems based on a semiconductor photocatalyst such as TiO_2, ZnO, etc., and a photon source, such as ultraviolet (UV) or sunlight, which generates highly powerful reactive radicals, including hydroxyl radicals ($HO^{\bullet}$) (E_0 = 2.8 V), holes (h^+), superoxide anion ($O_2^{\bullet -}$) and hydroperoxyl ($HO_2^{\bullet}$) [14,15]. TiO_2 (~3.2 eV) and ZnO (~3.37 eV) are widely used functional semiconductors that are chosen for their low cost, chemical stability, non-toxicity, and higher photosensitive properties [16–18]. Under irradiation with a light source ($h_v \geq E_g$), free electrons and holes are generated in the conductive and valence bands of the semiconductor (e^-_{CB}/h^+_{VB}) [19,20]. Hence, the degradation and mineralization of organic pollutants in water systems into carbon dioxide, water, and mineral salts is improved [21,22]. In recent years, sonocatalysis (SC) (US/TiO_2) has become a popular AOP. SC is based on the generation of huge amounts of $OH^{\bullet}$ radicals due to the collapse of cavitation bubbles driven by ultrasound [23]. Ultrasonic splitting of water molecules and electron activity on the catalyst surface (TiO_2 and ZnO) oxidize organic pollutants when catalysts are exposed to UV irradiation, according to the following equations [24,25]:

$$\text{Catalyst} \xrightarrow{h\upsilon} \text{catalyst}\left(e^-\right) + \text{catalyst}\left(h^+\right) \quad (1)$$

$$h^+ + OH^-_{ads} \rightarrow {}^{\bullet}OH \quad (2)$$

$$e^- + O_2 \rightarrow O_2^- \rightarrow {}^{\bullet}OH \quad (3)$$

$$H_2O \xrightarrow{))))} {}^{\bullet}H + {}^{\bullet}OH \quad (4)$$

$${}^{\bullet}OH + {}^{\bullet}OH \rightarrow H_2O_2 \quad (5)$$

where h^+ is a hole, and e^- is an electron [24]. The coupling of sonocatalysis (SC) and photocatalysis (PC), dubbed "sonophotocatalysis" (SPC; US/UV/TiO_2) is mainly responsible for the generation of active radicals and enhancement of the degradation efficiencies of organic and non-biodegradable recalcitrant pollutants [26]. The advantages of this "hybrid SPC process" could be summarized in the following: generation of more free radicals $^{\bullet}OH$ with strong oxidizing capability, enhancement of the catalyst's surface area, increasing the mass transfer to the liquid–solid interface, cleaning the catalyst surface, uniform distribution of a powdered form of catalyst in the liquid medium, regeneration of catalyst surface by turbulence, shear stress and micro-streaning, and enhancement of adsorption capacity of the catalyst [12,27–30]. Additionally, the hybrid SPC process is reported to increase the degradation efficiency of target pollutants in water/wastewater systems compared to the individual processes, and their combination is expected to reduce the operation cost, amount of reagent, operating time, and energy requirements for mineralization of pollutants in the engineering aspect [24,30–32]. Although the treatment of carpet washing wastewater (CWW) has been studied with various individual processes in the literature [1,2,4,5,33,34], no one has attempted to understand the hybrid degradation effects of ultrasound (US) and photocatalysis (PC) on the treatment of CWW. Besides, various independent factors such as pH, catalyst type and concentration, operation time, and H_2O_2 concentration have a significant impact on hybrid AOP performances that were reported especially for the treatment of several industrial wastewaters. Poblete et al. [35] discussed the synergistic effect of heterogeneous photocatalysis (HP) and ultrasound (US) to treat pisco vinasse, dark brown wastewater with high polyphenols contents and COD over 60 min treatment period. The efficiency of hybrid HP + US treatment was attained as the best removal ratios for polyphenols (68%), COD (70%), and color (48%) under 36 W UVC_{254} irradiation with 37 kHz and 500 W US system. Furthermore, [24] declared that 59% COD removal from real olive mill wastewater was achieved within 90 min in the US/UV/TiO_2 system. Also, the effect of various operating parameters such as, ultrasound power, initial COD concentration, the concentration of TiO_2, frequency of ultrasound, and temperature on the OMW oxidation efficiency was discussed based on the conventional one variable determination method independently at a specific time while keeping other factors constant. The maximum COD removal rate was achieved at 0.75 g/L of TiO_2 at frequency of 20 kHz. However, the operational costs, required time, and number of experiments can be reduced by using a statistical design method that optimizes operational conditions for the maximum removal efficiency [36,37]. In this work, as a first time, Taguchi multivariate optimization technique was used to analyze the most effective operation parameters from the key factors by hybrid SPC method to treat a real industrial wastewater. Furthermore, the contribution percentage of each factor on SPC process could be determined by this method for the maximum COD and color removal from CWW. In addition, the energy cost of SPC and the synergistic effects among individual AOPs could be assessed to gain insight on the applicability of the hybrid treatment method to this type of wastewater.

This study presents great originality and novelty for certain reasons: (i) the sonophotodegradation of CWW was performed for the first time with anatase nanosized TiO_2 and ZnO catalysts; (ii) to the best our knowledge, it would be one of the limited hybrid SPC treatment studies on the treatment of real industrial wastewater as compared with literature; (iii) catalyst type, catalyst concentration, and varied operation conditions were optimized, and efficient

AOP for mineralization and color removal of CWW were demonstrated in a short operation time; (iv) secondary pollutants, such as a sludge or high concentrations of anions as in the Fenton process were not formed during the operation; (v) a fast, technically high-efficiency, and economical treatment was proposed to reduce pollution load in wastewater from such facilities that direct high amounts of water to the urban water treatment plant.

2. Materials and methods

2.1. Chemicals

The nanopowder TiO_2 (AEROXIDE® P25 ≥ 99.5%, anatase form, 21 nm, 35–65 m^2/g BET surface area) was supplied by Sigma-Aldrich (Germany). Zinc oxide (ZnO) is the other nanopowder photocatalyst (<5 μm particle size, 99.9%; <10–25 m^2/g) supplied by Sigma-Aldrich (Germany) that was selected in this study. Hydrogen peroxide solution (30%, H_2O_2) was used as an oxidant, provided by Sigma-Aldrich (Germany). Sodium hydroxide (NaOH, 99%) and sulfuric acid (H_2SO_4, 97%) were procured from Merck (Germany). All chemicals were used without additional purification. During the experiments, deionized water was used to prepare the necessary solutions (Merck Milli-Q, Germany, spec. resistivity: 18.2 MΩ).

2.2. Carpet washing wastewater

The CWW used in this study was supplied by a local carpet washing company located in the city center of Bolu in Turkey. The CWW was sampled as composite for 2 h and collected from the effluent of the washing system. The CWW was kept in amber bottles at 4°C in the dark. The fundamental physico-chemical characterization of CWW samples is given in Table 1.

Table 1
Physico-chemical characteristics of carpet washing wastewater (CWW)

Parameter	Value
pH	7.49 ± 0.03
Temperature, °C	21.97 ± 0.06
Redox potential, mV	21.83 ± 0.25
Electrical conductivity, μS/cm	486.63 ± 0.15
Turbidity, NTU	175.33 ± 2.52
Color, mg/L	1,150.33 ± 1.53
Suspended solids, mg/L	74.00 ± 1.00
COD, mg/L	795.67 ± 0.58
NH_4–N, mg/L	19.50 ± 0.50
NO_2–N, mg/L	1.04 ± 0.02
NO_3–N, mg/L	5.17 ± 0.15
PO_4–P, mg/L	7.95 ± 0.05
Appearance	Brown
Sulfate, mg/L	17.52 ± 0.46
BOD, mg/L	138.72 ± 0.36
Anionic active substance (%)	0.08 ± 0.01
Cationic active substance (%)	<0.066

Data represent the mean ± standard error of three replicates.
COD – Chemical oxygen demand; BOD – Biochemical oxygen demand.

2.3. Reactor design

All ultrasound, photocatalytic, and sonophotocatalytic experiments were performed using the same cylindrical Pyrex glass immersion well reactor filled with 200 mL solution with certain amount of catalyst. The batch-mode reactor equipped with a water jacket and a PL-L UVA lamp (Philips, Dutch) (36 W; 315–38 nm; 110 μW/cm^2) was used to study the SPC method (Fig. 1). Air at 3.5 L/min was supplied to the reactor system using a diffuser. For the US experiments, the whole photoreactor system was immersed into an ultrasonic bath (Bandelin DT 106, Germany) with a capacity of 5.6 L (operating volume, 200 mL), a tank size of D = 240 mm and L = 125 mm, and an operating frequency of 35 ± 3 kHz (120 W, 220 V). The reactor temperature was kept constant at 25°C ± 3°C with the help of suitable cooling equipment.

2.4. Experimental conditions

CWW samples were taken at the beginning and end of each experiment run, centrifuged at 5000 rpm for 15 min, and filtered using 0.45 μm filters (Minisart RC25, Sartorious) to remove catalysts. COD and color values before and after treatment were determined by standard methods [38] using a Merck Pharo100 spectrophotometer (Germany). The COD was measured using commercial test kits (COD Merck 1.14541, 25–1,500 mg/L Spectroquant test kit). A 3 mL sample was measured over 120 min at 150°C under thermoreactor Spectroquant TR 320 (Merck, Germany) treatment. When the sample contained hydrogen peroxide (H_2O_2), interference in COD determination was reduced by increasing the pH to above 10 to decompose the hydrogen peroxide to oxygen and water [39]. Each experiment was performed in duplicate, and the average results are given in this study. Removal efficiency of pollutants was calculated using Eq. (6) [40]:

$$\text{Removal efficiency}\left(Y\right)=\left(\frac{C_0-C}{C_0}\right)\times 100 \tag{6}$$

where Y defines the removal efficiencies of COD and color; C_0 and C represent initial and final pollutant concentrations, respectively.

2.5. Experimental design

Taguchi method is a multivariable optimization technique that is used to define and optimize key design parameters in a shortened experimental period with a minimum number of trials [41]. After a number of preliminary experiments, a two-level and three-level Taguchi method based on five independent parameters (catalyst type (x_1), initial dosage (g/L) of catalyst concentration (x_2), pH (x_3), initial dosage (mmol/L) of H_2O_2 concentration

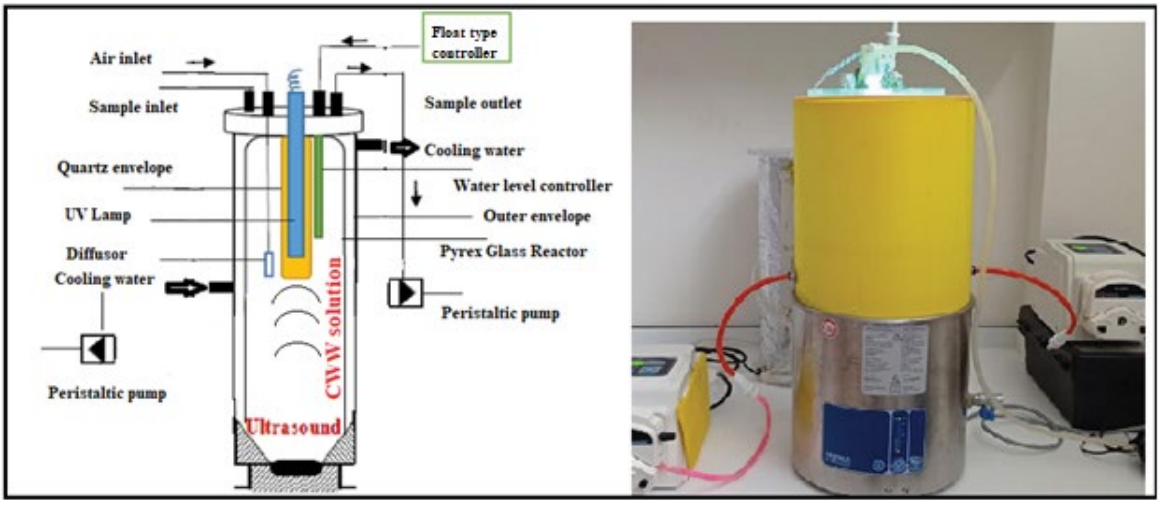

Fig. 1. Experimental set-up for the hybrid sonophotocatalysis (SPC) system.

(x_4) and time (min) of operation (x_5)) were designed to model the process. Table 2 gives the fundamental operation parameters and their levels. Recently, experiments have been frequently designed and optimized in Taguchi method by the systematic orthogonal array (OA). The OA is conducted with the largest number of variables and the least number of experiments [42]. The Taguchi L_{18} ($2^1 \times 3^4$) OA was selected as the best fitting to determine the optimum COD and color removal for investigating the effects of the SPC process parameters. The Minitab software (version 17-trial edition) was used to calculate the experimental data.

Signal-to-noise (S/N) ratio is a widely used optimization criterion that was selected as the performance indicator in the Taguchi design. The usually used S/N ratio functions are "The smaller is better," "The nominal is better," and "The larger is better." "Larger is better" was selected to achieve higher removal efficiencies using SPC process. The related S/N ratio is calculated using Eq. (7) [43]:

$$\frac{S}{N}\left[dB\right] = -10\log\left[\frac{1}{n}\sum_{i=1}^{n}\frac{1}{Y_i^2}\right] \tag{7}$$

where n defines the number of the experimental replications and Y_i is the performance value of the ith experiment.

The balanced characteristic of OA can be used to predict the performance values related to the optimum conditions that are given in Eq. (8):

$$Y_i = m + X_i + e_i \tag{8}$$

where m is defined as the overall mean of the performance value, X_i is defined as the fixed effect of the parameter level combination used in the ith experiment, and e_i is defined as the random error in the ith experiment [44].

Ω transformation of percentage values is used when the experimental results are in percentage (%), using Eq. (9). Then, reverse transformation is carried out using the same equation to determine values of interest [45]:

$$\Omega\ \left(db\right) = -10\log\left(\frac{1}{P} - 1\right) \tag{9}$$

where Ω (db) is defined as the decibel value of percentage value subject to omega transformation, and P is defined as the percentage of product obtained experimentally ($0 < p < 1$) [46].

3. Results and discussion

3.1. Preliminary studies

Various individual (UV, US, TiO_2, ZnO, and H_2O_2) and hybrid (UV + US, US + TiO_2, UV + TiO_2, US + ZnO, UV + ZnO, US + UV + TiO_2, and US + UV + ZnO) advanced oxidation processes (AOPs) were studied to provide the oxidation potential as COD removal (%) and color of CWW under the same operation conditions as shown in Table 3.

CWW COD levels indicated that individually, UV, US, and H_2O_2 cause negligible reduction, and CWW color levels indicated that the individual US and UV methods cause negligible reduction. H_2O_2 enables reduction of the color of CWW due to producing extra •OH, which also advances the degradation of pollutants, especially dyes [47]. Table 3 indicates that the oxidation of CWW using UV combined with US was only 22% vs. 41% under UV + US + TiO_2 process at the end of 180 min. Yet, only 34% oxidation of CWW was obtained after under UV + US + ZnO process after treatment for 180 min.

The synergy index is the ratio of the hybrid SPC removal percentage value to the sum of the individual processes' removal percentage values with regards to COD removal. The index was calculated to present the strength contributions from US, UV-TiO_2 and UV-ZnO processes. For the oxidation of CWW, the observed synergy index values for the combined UV + US + TiO_2 and UV + US + ZnO were obtained as 1.46 and 1.50, respectively. Poblete et al. [35] reported lower synergy level (0.99) for the treatment of vinasse with US-UV/TiO_2 for COD removal. However, Sunasee et al. [48] declared that in terms of synergy index,

Table 2
L_{18} orthogonal array for Taguchi experimental design

Parameters	Symbol	Level 1	Level 2	Level 3
Catalyst type	*A*	TiO_2	ZnO	–
Catalyst concentration (g/L)	*B*	0.5	1.5	2.5
pH	*C*	2	6	10
H_2O_2 concentration (mmol/L)	*D*	0	5	10
Time (min)	*E*	30	105	180

Table 3
COD and color removal efficiencies resulting from using a variety of individual and combined processes (35 kHz US frequency; 120 W US power; pH 10.0; 1.5 g/L catalyst concentration; 36 W UV power; 25°C ± 3°C temperature)

Advanced oxidation treatment methods (AOPs)	COD removal (%)	Color removal (%)
Ultraviolet (UV)	7.5 ± 0.39	5.77 ± 0.38
Ultrasound (US)	3.22 ± 0.55	14.6 ± 0.46
TiO_2	20.8 ± 0.54	83.6 ± 0.71
ZnO	16.6 ± 0.34	84.5 ± 0.67
H_2O_2	9.6 ± 0.34	85.5 ± 0.55
UV + US	21.9 ± 0.24	84.7 ± 0.08
US + TiO_2	24.5 ± 0.51	81.1 ± 0.96
UV + TiO_2	27.5 ± 0.59	83.5 ± 0.37
US + ZnO	18.4 ± 0.47	81.7 ± 0.12
UV + ZnO	19.3 ± 0.70	82.2 ± 0.01
UV + US + TiO2	**40.5 ± 0.66**	**95.2 ± 0.24**
UV + US + ZnO	**33.8 ± 0.09**	**89.5 ± 0.37**

Data are shown as mean ± standard error of three replicates.

the synergistic effect of the combination of US/UV/P25 to remove Bisphenol A (BPA) was found to be 2.2 indicates a positive effect. Kakavandi and Ahmadi [49] reported that if integrated effect was equal to sum of the individual effects, an additive effect occurred and the value of *R* is equal to 1 and $R > 1.0$ indicates a synergistic effect. This means that the combination of photocatalysis and ultrasound processes achieved higher oxidation performance of CWW when compared with individual processes. The reason for the efficient treatment performance of hybrid SPC was thought to be the prevention of suspended catalyst nanosized agglomerations due to the propagation capability of ultrasound throughout the method. Hence, the surface area of catalysts was increased, which resulted in increased generation of additional free •OH radicals due to this effect in the reaction mixture [24]. Besides, the catalyst surface could be cleaned continuously by the ultrasonic waves, preventing pollutant accumulation and that of their intermediates produced during degradation [30].

3.2. Taguchi analysis to determine optimum parameters

Taguchi analysis was performed to define the optimal parameters and to determine the parameters having the most significant effect on the COD and color removal from CWW [50]. Table 4 presents the experimental and predictive S/N and mean values of COD and color removal efficiencies via Taguchi L_{18} ($2^1 \times 3^4$) OA that was used for the examination of the effects of five factors with three levels. Each run of the matrix indicates one test run.

Table 4 indicates the maximum removal efficiencies were obtained in experiment 4 for COD removal, whereas experiment 3 indicated the highest color removal efficiency. A Taguchi-based response table was used to determine the most effective process parameters among catalyst type, catalyst concentration, operation pH, H_2O_2 concentration, and operation time for the optimal levels of COD and color removal efficiencies. According to the S/N table shown in Table 5, catalyst concentration was the highest effective parameter the COD removal and pH and operation time as the most effective on the color removal.

The optimum conditions were A1, B2, C1, D1, and E3 for COD removal and A2, B1, C3, D3, and E3 for color removal. Fig. 2 illustrates the main effects plot for S/N ratios in the evaluation of COD and color reduction in SPC process. As shown in Fig. 2a, S/N ratios showed that optimal parameters (highest values) for COD removal were the 1st level (A1-TiO_2) of catalyst type, the 2nd level (B2-1.5 g/L) of catalyst concentration, the 1st level (C1-2) of pH, the 1st level (D1-0 mmol/L) of H_2O_2 concentration, and the 3rd level (E3-180 min) of time. Further, as shown in Fig. 2b, the optimal parameters (highest values) for color removal were the 2nd level (A2-ZnO) of catalyst type, the 1st level (B1-0.5 g/L) of catalyst concentration, the 3rd level

Table 4
Experimental structure and average results Taguchi L_{18} ($2^1 \times 3^4$)

						COD removal percentage (%)				Color removal percentage (%)			
Exp. No.	Factor *A*	Factor *B*	Factor *C*	Factor *D*	Factor *E*	S/N (dB)	Mean value	Predictive S/N (dB)	Predictive mean value	S/N (dB)	Mean value	Predictive S/N (dB)	Predictive mean value
1	1	1	1	1	1	32.96	44.46	32.38	43.08	39.28	92.05	39.15	90.81
2	1	1	2	2	2	31.16	36.12	30.68	35.90	38.81	87.23	38.71	86.16
3	1	1	3	3	3	28.05	25.28	28.45	25.98	39.91	**99.00**	39.88	98.56
4	1	2	1	1	2	34.55	**53.38**	34.86	53.06	38.74	86.52	38.84	87.42
5	1	2	2	2	3	33.87	49.36	33.34	46.13	38.82	87.27	38.79	86.96
6	1	2	3	3	1	30.45	33.29	30.23	33.54	39.29	92.13	39.31	92.47
7	1	3	1	2	1	33.24	45.92	33.21	45.44	38.96	88.76	39.02	89.32
8	1	3	2	3	2	28.44	26.43	28.95	28.59	38.53	84.44	38.69	86.05
9	1	3	3	1	3	31.58	37.93	32.19	40.43	39.29	92.16	39.25	91.82
10	2	1	1	3	3	28.53	26.70	27.71	23.63	39.74	97.06	39.86	98.27
11	2	1	2	1	1	27.09	22.63	28.22	26.11	38.54	84.52	38.66	85.69
12	2	1	3	2	2	28.00	25.13	28.36	25.62	39.29	92.13	39.32	92.51
13	2	2	1	2	3	31.61	38.05	32.68	43.36	39.32	92.47	39.34	92.71
14	2	2	2	3	1	27.62	24.05	27.73	24.08	38.87	87.78	38.76	86.75
15	2	2	3	1	2	31.53	37.73	30.79	35.68	38.94	88.46	38.92	88.33
16	2	3	1	3	2	28.26	25.89	28.30	25.82	39.41	93.48	39.25	91.80
17	2	3	2	1	3	30.42	33.20	29.69	30.98	38.74	86.46	38.70	86.10
18	2	3	3	2	1	29.53	29.96	29.13	28.06	39.08	90.00	39.11	90.22

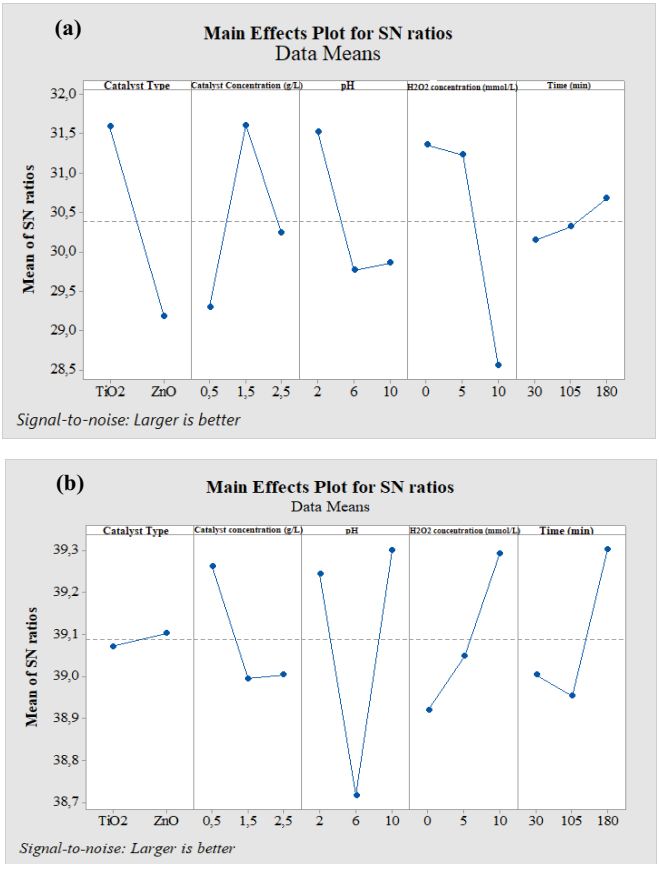

Fig. 2. Factor levels effect on S/N ratio for (a) COD removal efficiency and (b) color removal efficiency.

(C3-10) of pH, the 3rd level (D3-10 mmol/L) of H_2O_2 concentration, and the 3rd level (E3-180 min) of time. As presented in Table 5, the highest COD and color removal were 53% and 99%, respectively, based on the obtained results. According to Table 5, the average COD removal efficiency from CWW is 53%, while the color removal efficiency is 99% because the color removal is probably due only to the breakdown of the chromophore groups of the dyes that give color to the wastewater, while extensive oxidation of the entire molecule is required for COD removal [51]. It is thought that the reason for the high color removal in CWW is the formation of intermediate products by the attack of •OH on CWW, and their reaction with •OH until complete mineralization is achieved [35]. Further, the reason for high color removal in CWW is thought to be the formation of intermediate products by the attack of •OH on CWW, along with their reaction with •OH until complete mineralization is achieved [35].

3.3. Effects of operating parameters on COD and color removal

3.3.1. Catalyst type and concentration effect

The effect of three catalyst dosages of 0.5, 1.5, and 2.5 g/L on the COD and color degradation was investigated for TiO_2 and ZnO catalysts. As shown in Figs. 2a and b and 3a and b, although catalyst type had a significant impact on COD removal, it was an insignificant factor in the color removal of CWW (Table 5). The nanosized TiO_2 particles have smaller particle size (21 nm) with a larger total surface area (35–65 m^2/g) than the ZnO catalyst (<5 μm particle size, 99.9%; <10–25 m^2/g). Thus, they provide more chances for the organic matter to adsorb on the catalyst surface [24]. The transient implosion of cavitation bubbles in the surroundings of the photocatalyst particles enables formation of more radicals that degrade pollutants [30]. Besides, it can be stated that TiO_2 shows better individual and combined oxidation for sonoluminescence induced by ultrasonic irradiation and excitation using UV irradiation. Greater generation of hydroxyl radicals in the hybrid process leads to higher oxidation rate and continuous cleaning on the catalyst surface for a longer period [52].

Catalyst concentration is a significant factor in both COD and color removal efficiency, as shown in Fig. 3a and b. Increasing TiO_2 catalyst concentration causes an increase in the number of cavitation bubbles due to providing additional nuclei, and consequently, more OH^- radicals are generated in the bulk solution (Fig. 2a). Also, the availability of active sites on the catalyst surface increases up to the optimum value (1.5 g/L of TiO_2) with an increase in catalyst loading [36,53]. However, at higher dosage (higher than 1.5 g/L for TiO_2 and 0.5 g/L for ZnO), more catalyst aggregation will occur that results with inhibition of light penetration, and the loss of active sites depends on shielding effects, generating OH^- in the solution. Further, excessive amounts of sonocatalyst lower the amount of ultrasonic waves passing into the solution [54,55]. The results are in good agreement with those obtained by [56], where COD reduction of real phosphonate-containing industrial wastewater increased from 48% to 64.9% with an increase in TiO_2 loading from 0.1 to 0.5 g/L, and consequently, a greater decrease was observed with an increase in catalyst loading.

3.3.2. pH effect

The pH plays an essential role in the generation of hydroxyl radicals and the chemical form of various organic pollutants in wastewater [25]. The change of pH value was investigated at pH levels 2, 6, and 10. In Fig. 4a and b, the effect of pH on the COD and color removal from CWW could be observed. Based on the results in Figs. 2a and 4a, as pH increased from 2 to 6, a marginal decrease was achieved in COD removal, and finally, the pH showed a tendency to increase slightly to 10. This trend should be explained by the following steps: the initial organic compounds in the CWW firstly decomposed into intermediates, forming organic acids which consequently are decomposed to carbon dioxide [57]. Secondly, the reason for the increase of COD removal in acidic conditions could probably be related to the point of zero charge (pH_{ZPC}) of TiO_2 catalyst (6.25) [58]. Under acidic conditions ($pH < pH_{ZPC}$), the surface of the catalyst (TiO_2) is positively charged from absorbing H^+ ions, and the pollutant molecules are negatively charged due to significantly high electrostatic attraction [59]. Similar to these findings, Dinesh et al. [60] confirmed that the enhanced formation of hydroxyl radicals influenced the efficiency of SPC at lower pH. When the initial pH of the solution changed from 6.04 to 2, degradation of basic brown 1 dye increased from 11% to 43% at 37 kHz ultrasound frequency. At lower pH, •OH radicals

Table 5
S/N response tables for COD and color removal efficiencies (%)

	COD removal (%)						Color removal (%)				
	Catalyst type	Catalyst concentration (g/L)	pH	H_2O_2 concentration (mM)	Time (min)		Catalyst type	Catalyst concentration (g/L)	pH	H_2O_2 concentration (mM)	Time (min)
Level	*A*	*B*	*C*	*D*	*E*	Level	*A*	*B*	*C*	*D*	*E*
1	**31.59**	29.3	**31.52**	**31.36**	30.15	1	39.07	**39.26**	39.24	38.92	39
2	29.18	31.6	29.77	31.23	30.32	2	**39.1**	39	38.72	39.05	38.95
3		30.25	29.86	28.56	**30.68**	3		39.00	**39.3**	**39.29**	**39.3**
Delta	2.41	2.3	1.76	2.8	0.53	Delta	0.03	0.27	0.58	0.37	0.35
Rank	2	3	4	1	5	Rank	5	4	1	2	3

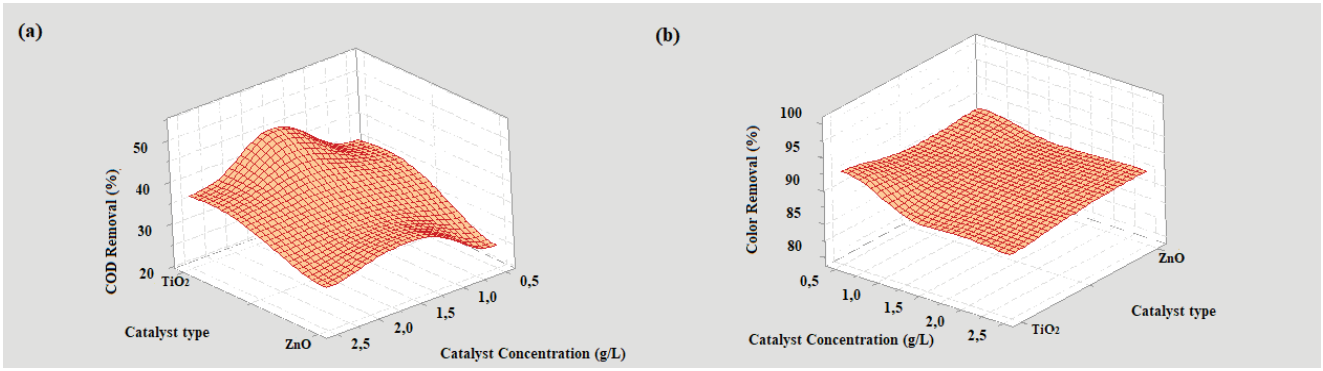

Fig. 3. Surface plots for catalyst concentration effect.

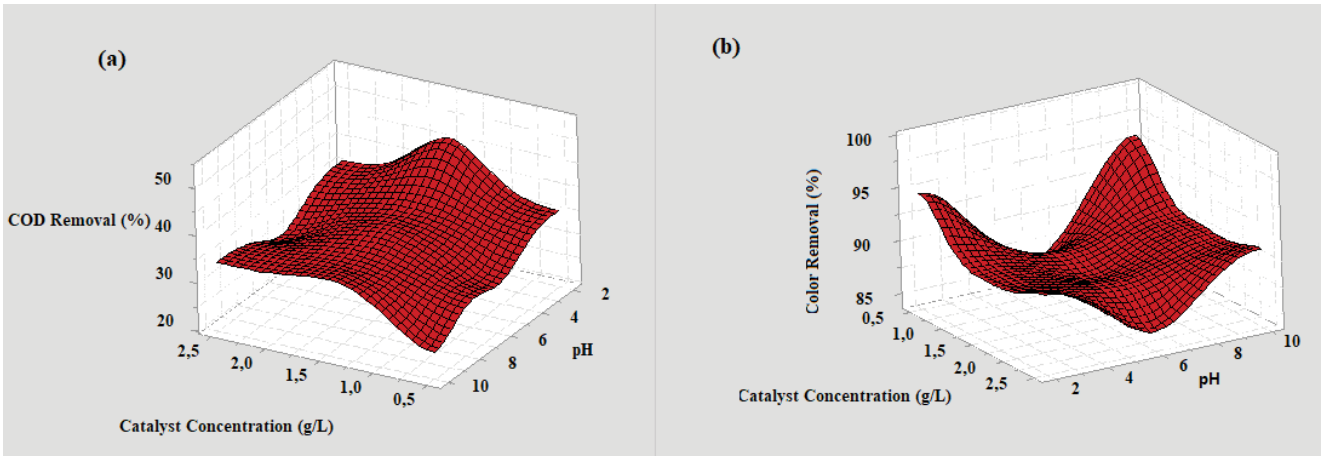

Fig. 4. Surface plots for pH effect.

are easily generated by oxidizing more hydroxide ions. Additionally, according to the Nernst equation [Eq. (10)], when the solution pH was declined, the redox potential of HO• radicals was increased. Thus, with increasing the pH amount from 2 to 6, the HO• redox potential theoretically decreased from 2.69 to 2.21. Ghanbari et al. [61] reported that the degradation of acetaminophen (ACM) was comparatively studied by UV/chlorine and UV/H_2O_2 systems and with increasing the pH amount from 7 to 11 the HO• redox potential theoretically decreased from 2.39 to 2.15. Hence, over 85% of the contaminant was removed at pH of 7.0 during 25 min of reaction time.

$$E^0 = E^0_{\bullet OH/H_2O} - 0.059\ pH \quad (10)$$

Moreover, color removal reached maximum at pH 10, as indicated in Figs. 3b and 4b. The point of zero charge (pH_{ZPC}) of ZnO is 9.0; hence, a positive charge on the sonocatalyst surface is formed by decreasing pH values (<9.0) [36].

3.3.3. H_2O_2 concentration effect

H_2O_2 is a powerful oxidizing agent that is added to the catalyst to increase the rate of photooxidation. Determination of the optimum dose of H_2O_2 according to the type and concentration of pollutants is vital to keep the efficiency of added H_2O_2. H_2O_2 concentrations of 0, 5, and 10 mmol/L of were investigated in this study to observe its effect on COD and color removal efficiency. A photogenerated electron is accepted by H_2O_2 from the conduction band of the catalyst, as follows in Eq. (11). Hence, charge separation is promoted. Besides, H_2O_2 forms •OH radicals, as given in Eq. (12) [62]:

$$e^- + H_2O_2 \rightarrow {}^\bullet OH + OH^- \quad (11)$$

$$H_2O_2 + {}^\bullet O_2 \rightarrow {}^\bullet OH + OH^- + O_2 \quad (12)$$

The addition of hydrogen peroxide enhances the color removal of CWW in the presence of ultrasound due to additional free radical generation from zero to 10 mmol/L of H_2O_2 (Fig. 5b). As illustrated in Fig. 5b, at higher and lower pH values, 10 mmol/L of H_2O_2 caused the highest color removal from CWW. However, with an increased H_2O_2 dosage from 5 to10 mmol/L, COD removal was decreased, as shown in Fig. 5a. This situation can be explained by excess H_2O_2 reacting with the hole and •OH to form $HO_2^\bullet$. This leads to hole scavenging that reduces oxidation efficiency, as indicated by Steven et al. [63] in Eqs. (13)–(15). Steven et al. [63] presented that peroxyl radicals were produced by the reaction of hydroxyl radicals

Table 6
ANOVA for COD and color removal

Variance source	Degree of freedom (DoF)	Sum of squares (SS)	Mean square (MS)	*F*-ratio	*p*-value	% Contribution (Cr)
COD removal						
A	1	438.305	438.305	40.3	0.000	**29.43%**
B	2	265.531	132.766	12.21	0.004	17.83%
C	2	214.080	107.040	9.84	0.007	14.37%
D	2	475.715	237.857	21.87	0.001	**31.94%**
E	2	8.74	4.37	0.4	0.682	0.59%
Error	8	87.008	10.876			5.84%
Total	17					100.00%
Color removal						
A	1	0.435	0.435	0.25	0.631	0.16%
B	2	32.252	16.126	9.22	0.008	11.68%
C	2	132.545	66.272	37.91	0.000	**47.98%**
D	2	48.845	24.422	13.97	0.002	17.68%
E	2	48.173	24.087	13.78	0.003	17.44%
Error	8	13.985	1.748			5.06%
Total	17					100.00%

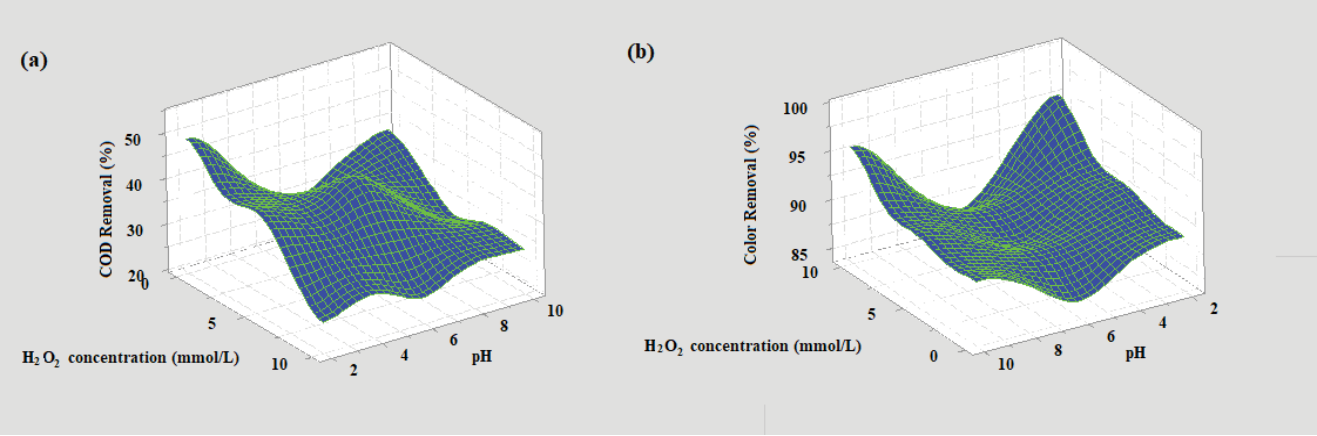

Fig. 5. Surface plots for H_2O_2 concentration effect.

with excess H_2O_2 [Eq. (13)]. The high amount of produced peroxyl radicals consume the •OH radicals [Eq. (14)] and dimerize back to H_2O_2 [Eq. (15)].

$$H_2O_2 + {}^{\bullet}OH \rightarrow HO_2^{\bullet} + H_2O \quad (13)$$

$$HO_2^{\bullet} + {}^{\bullet}OH \rightarrow H_2O + O_2 \quad (14)$$

$${}^{\bullet}OH + {}^{\bullet}OH \rightarrow H_2O_2 \quad (15)$$

3.3.4. Operation time effect

As illustrated in Fig. 6a and b, when the operation time of SPC process increased from 30 to 180 min, a non-significant increased trend in COD removal was achieved, while the color removal performance reached a maximum at 180 min. According to the main findings of this research, it is thought that high operating time is required to remove both the recalcitrant target compounds and the intermediates to be obtained by the breakdown of these products. Similar to the results of this study, Soltani et al. [36] used 2 g/L bentonite-supported ZnO catalyst in the treatment of real textile wastewater, achieving 44% COD removal efficiency at the end of 150 min operation time. They emphasized that a long reaction time is necessary in real wastewater treatment. Bullo et al. [64] reported that the photodegradation of methylene blue from synthetic wastewater took longer time (180 min) to reach full degradation by calcinated eggshell (CES) doped with TiO_2.

Similarly, Soltani and Safari [65] stated in their study that a continuous increase in OH^- radicals in the aqueous phase, depending on the increase in sonication time, with

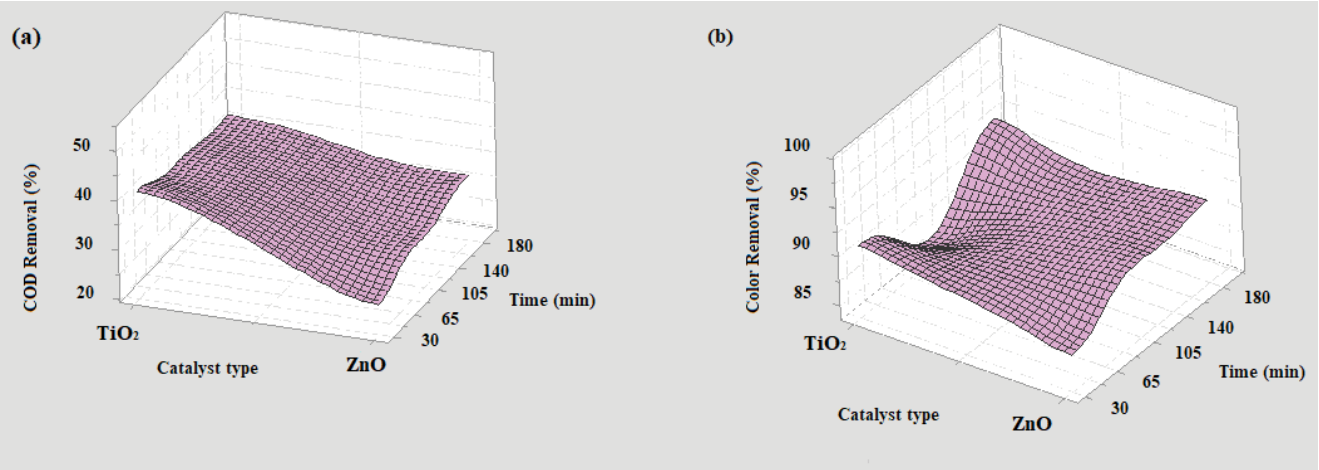

Fig. 6. Surface plots for operation time effect.

the occurrence of cavitation, is effective in the sonocatalytic degradation of organic dye molecules.

3.4. Analysis of variance and regression analysis

The factors that significantly affect the response parameters and evaluation of their individual interactions on the COD and color removal efficiencies were determined by performing analysis of variance (ANOVA). The ANOVA results stated the effects on COD and color removal efficiencies of the controllable catalyst type and concentration, pH, H_2O_2 concentration, and operation time in the SPC process at a confidence level of 95% and a significance level of $\alpha = 0.05$, as presented in Table 6. The significance of the parameters is represented by the *p*-values that are lower than 0.05 ($p < 0.05$). *F*-ratio states the parameters that have a significant effect on COD and color removal by SPC process. As given in Table 6, the errors were 5.84% and 5.06% (<50%), respectively, for COD and color removal, which were well below the limit value. This implied that the errors of the experiments were insignificant. According to the results, the highest *F*-ratio (40.3) was catalyst type, and the operation time was statistically insignificant ($F = 0.4$, $p = 0.682$, $p > \alpha$) for COD removal. Besides, the variance in pH had the most significant effect on color removal, while catalyst type had an insignificant effect on color removal. The qualitative assessment of factorial effects is provided by using *F*-ratios in ANOVA for the Taguchi method. However, quantitative assessment can be obtained using percentage contribution rate (Cr%) [66]. The contribution ratio can be computed by dividing the source's net variation by SS_T as given in Eq. 16.

$$\mathrm{Cr}_A = \frac{\mathrm{SS}_A - \mathrm{DOF} \times \mathrm{MSS}_{\mathrm{error}}}{\mathrm{SS}_{\mathrm{total}}} \times 100 \tag{16}$$

In Table 6, ANOVA results report Factor *D* (H_2O_2 concentration) is the most effective parameter for COD removal, with a contribution ratio of 31.94%. Factor *A* (catalyst type) was the most significant parameter after H_2O_2 concentration at 29.43%. Factor *E* (operation time) was the least significant factor for COD removal. For color removal, the most significant parameter was pH (Factor *C*) at 47.98% contribution rate, but other factors (Factor *A*, 0.16%; Factor *B*, 11.68%; Factor *D*, 17.68% and Factor *E*, 17.44%) had less significant effects on color removal. Moreover, the R^2 and adjusted R^2 values were 0.9416 and 0.8759 for COD removal and 0.9494 and 0.8924 for color removal, respectively. In all cases, these confirm a good correlation between predicted and experimental results.

Regression analysis denotes modeling or analysis of a mathematical relationship between one or multiple process variables (continuous predictors) and the response (COD and color removal). Regression analysis was used in this this study to compute the equations for prediction of COD and color removal efficiencies [67]. Linear models were formulated by equation predictions as shown in Table 7, and the R^2 values obtained via linear regression model equations were 69.05% and 37.03% for COD and color removal, respectively.

As illustrated in Fig. 7, the predicted COD and color removal efficiency values correlated well with the experimental results, with 94.2% and 95.3% R^2 values for COD and color removal, respectively. The quadratic regression model produced more comprehensive predicted values and exhibited better performance than the linear regression model [68].

3.5. Confirmation test

The obtained optimum parameters were used in confirmation experiments, and the results were compared with the predicted results from the linear regression model, which are given in Table 8 [69]. The difference between the observed Y_i and the predicted Y_i gives the prediction error. The confidence interval calculation is defined in the following equation [70]:

$$S_e = \pm 2\sqrt{\left[\frac{1}{n_0}\right]\sigma_e^2 + \left[\frac{1}{n_T}\right]\sigma_e^2} \tag{17}$$

Table 7
Linear regression models by equation prediction of COD and color removal efficiency

COD removal (%)
TiO_2 (linear) = 46.84 + 1.58 Catalyst concentration (g/L) – 0.939 pH – 1.128 H_2O_2 concentration (mmol/L) + 0.0113 min
ZnO (linear) = 36.97 + 1.58 Catalyst concentration (g/L) – 0.939 pH – 1.128 H_2O_2 concentration (mmol/L) + 0.0113 min
Color removal (%)
TiO_2 (linear) = 87.38 – 1.39 Catalyst concentration (g/L) + 0.074 pH + 0.396 H_2O_2 concentration (mmol/L) + 0.0213 Time (min)
ZnO (linear) = 87.38 – 1.39 Catalyst concentration (g/L) + 0.074 pH + 0.396 H_2O_2 concentration (mmol/L) + 0.0213 Time (min)

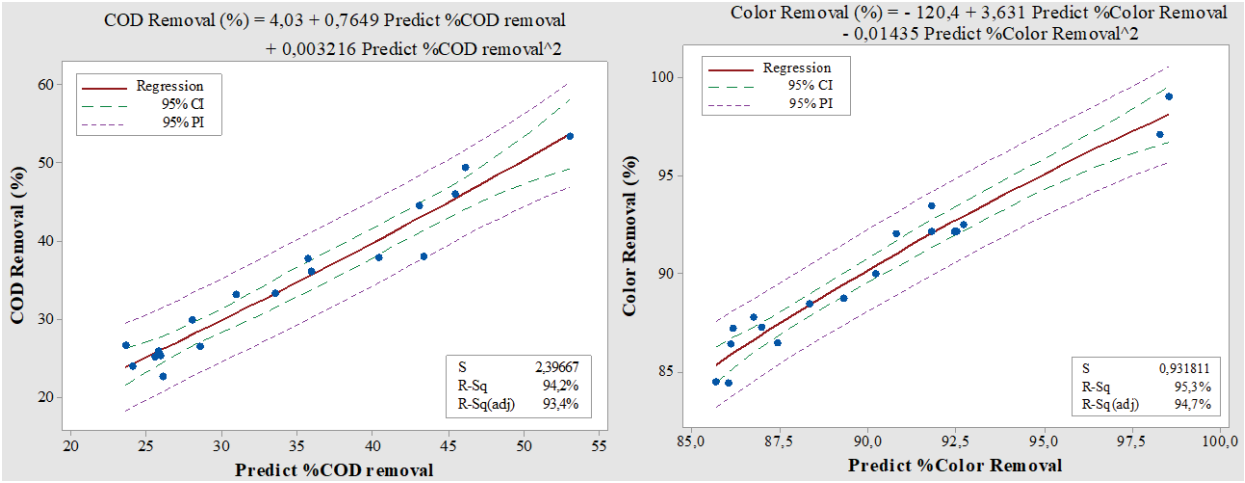

Fig. 7. Quadratic regression model compared with experimental results for COD and color removal (%).

$$\sigma_e^2 = \frac{\text{sum of squares due to error}}{\text{degrees of freedom for error}} \tag{18}$$

$$\frac{1}{n_0} = \frac{1}{n} + \left[\frac{1}{n_{A_i}} - \frac{1}{n}\right] + \left[\frac{1}{n_{B_i}} - \frac{1}{n}\right] + \left[\frac{1}{n_{C_i}} - \frac{1}{n}\right] \cdots \tag{19}$$

where S_e is defined as the confidence limit of the two-standard deviation; n is defined as the number of rows in the matrix experiment; n_r is defined as the number of repetitions in the confirmation experiment; and nA_i, nB_i, nC_i, … are the replication numbers for the parameter levels A_i, B_i, C_i, … The additive model is adequate if the prediction error is inside these limits [71,72]. The optimum parameters for the confirmation experiment results are exhibited in Table 8. The confirmation experiment results in Table 8 demonstrate that experimentally observed results were within the confidence intervals (within ±5% in error).

3.6. Energy cost comparison

Treatment cost is the most crucial engineering issue that directly influences the selection of a suitable treatment technique for the purification of industrial wastewater. In this work, cost of energy consumed (based on each mg COD removed from water) was considered for the individual and hybrid methods. The electricity price was assumed to be 0.0502 $/kWh in Turkey, which is used in Eq. (20) [73]:

$$\text{Cost of energy}\left(\frac{\$}{\text{kWh}}\right) = \frac{t(h)\times\sum P_i(\text{kW})\times\text{price of each power unit}\left(\frac{\$}{\text{kWh}}\right)}{R(\%)\times C_0\left(\frac{\text{mg}}{\text{L}}\right)\times V(L)} \tag{20}$$

where P_i is the power (kW) required by the equipment needed (ultrasonic power: 0.12 kW, light source power: 0.036 kW, air pump power: 0.003 kW) for each process (US, PC, UV, etc.) during the operation time t (h). C_0 can be defined as the initial COD concentration in CWW (mg/L); R is the removal efficiency (%); and V is the volume of treated water (L). As summarized in Table 9, the cost of energy consumed for the individual and hybrid processes was calculated taking COD removal into consideration. The optimum operation time and working volume were 180 min and 0.2 L, respectively.

Based on Table 9, US treatment had the highest energy requirement when tested individually. But when combined with catalysts and UV, the energy cost decreased. Photocatalysts that could trigger photochemical reactions would be the main reason for this increased efficiency. It could provide better removal of organic contaminants, resulting from the increased energy efficiency of the treatment process [44]. When the lower energy costs and high

Table 8
Confirmation experiment results for SPC process

		Parameters					Predicted	Observed	Confidence interval
		A	*B*	*C*	*D*	*E*			
COD removal percentage (%)	Level	1	2	1	1	3	49.37	53.38	40.06–58.68
	Value	TiO_2	1.5	2	0	180			
Color removal percentage (%)	Level	2	1	3	3	3	95.22	97.06	81.27–100.0
	Value	ZnO	1	10	10	180			

Table 9
Cost of energy for COD removal using each treatment method

Process	Cost (¢/kWh)
US	0.00430
UV	0.00061
US-UV	0.00082
UV/TiO_2	0.00018
UV/ZnO	0.00023
US/TiO_2	0.00063
US/ZnO	0.00075
US-UV/TiO_2	0.00032
US-UV/ZnO	0.00039

pollutant removal efficiencies of combined ultrasound (US) and photocatalysis (UV/catalyst) treatments are considered, it could be concluded that hybrid AOPs are a feasible option for treating CWW.

4. Conclusion

In the current study, for the first time, an energy efficient, environmentally friendly, and hybrid ultrasonic and photocatalytic process was designed and operated to treat organic pollutants and color from carpet cleaning wastewater. The other key outcomes could be drawn as follows:

- The hybrid sonophotocatalytic technology was more efficient in the removal of COD and color than using the individual AOPs such as US, UV, and H_2O_2 in the presence of catalyst (TiO_2 and ZnO nanoparticles) due to the higher amount of •OH radicals generated. Decolorization is much more efficiently achieved than COD removal.
- The optimum conditions obtained from Taguchi experiments for SPC process are as follows: 1.5 g/L TiO_2 at pH 2, 180 min for COD removal; for color removal, they are 0.5 g/L ZnO at pH 10, with 10 mmol/L of H_2O_2, and 180 min. With these optimum conditions, the actual removal efficiency for COD and color were 53% and 99%, respectively. The predicted removal percentages for COD and color obtained using regression model were 49.37% and 95.22%, respectively. The contribution rate (C_r) of catalyst type and H_2O_2 concentration have the highest effects on COD removal. Further, pH is the strongest parameter in color removal.
- The lowest energy cost calculated for hybrid US-UV/TiO_2, UV-TiO_2, and UV-ZnO were 0.00032, 0.00018, and 0.00023 ¢/kWh, respectively, to remove COD from CWW.
- Consequently, this hybrid treatment technology is very advantageous in that CWW can maintain a low level of pollutant concentration, which is limited in treatments with AOP, due to its low COD value and inclusion of a small amount of organic pollutants. Furthermore, there is no need for dilution water to dilute the waste concentration. Consequently, less experiments, short time and low energy cost are the fundamental advantages in this approach to attain targeted CWW treatment.
- As the majority of the earlier investigations in this area are based on a laboratory scale operation due to limited processing capacities, unsatisfactory performance in real conditions, mass transfer limitations, higher residence time necessities and inherent kinetics of advanced oxidation processes. Secondly, the economic sustainability of SPC wastewater treatment on a large scale is another critical challenge that should be discussed in terms of cost of the sonophotocatalyst and electrical energy consumptions especially for higher ultrasound frequencies. However, works in more realistic conditions (i.e., sunlight, etc.) at pilot-scale systems will add useful information in terms of successful implementation of hybrid sonophotocatalytic oxidation process for the real industrial wastewater treatment. Thus, further studies need to apply this new hybrid system for pilot-scale wastewater treatment and large-scale marketing.

Acknowledgements

Simge Dalkılıc is gratefully acknowledged by the author for her invaluable help in sampling wastewater and running experiments.

References

[1] F.A. Nasr, I. Abdelfattah, A.M. Shana, Cost-effective physico-chemical treatment of carpet industrial wastewater for reuse, Egypt. J. Chem., 62 (2019) 609–620.
[2] E. Shakeri, M. Mousazadeh, H. Ahmadpari, I. Kabdaşlı, H.A. Jamali, N.S. Graça, M.M. Emamjomeh, Electrocoagulation-flotation treatment followed by sedimentation of carpet cleaning wastewater: optimization of key operating parameters via RSM-CCD, Desal. Water Treat., 227 (2021) 163–176.
[3] C.G. Joseph, Y.H. Taufiq-Yap, N.A. Affandi, J.L.H. Nga, V. Vijayan, Photocatalytic treatment of detergent-contaminated wastewater: a short review on current progress, Korean J. Chem. Eng., 39 (2022) 484–498.

[4] S. Saroj, L. Singh, S.V. Singh, Photodegradation of Direct Blue-199 in carpet industry wastewater using iron-doped TiO_2 nanoparticles and regenerated photocatalyst, Int. J. Chem. Kinet., 51 (2019) 189–205.
[5] H. Cüce, Ş.M. Yakut, E. Özak, Treatment of carpet washing wastewater with an advanced oxidation process, BEU J. Sci., 7 (2018) 339–348.
[6] G. Fan, S. Yang, B. Du, J. Luo, X. Lin, X. Li, Sono-photo hybrid process for the synergistic degradation of levofloxacin by $FeVO_4$/$BiVO_4$: mechanisms and kinetics, Environ. Res., 204 (2022) 112032, doi: 10.1016/j.envres.2021.112032.
[7] K. Fouad, M. Bassyouni, M.G. Alalm, M.Y. Saleh, Recent developments in recalcitrant organic pollutants degradation using immobilized photocatalysts, Appl. Phys. A, 127 (2021) 612, doi: 10.1007/s00339-021-04724-1.
[8] J.O. Adeyemi, T. Ajiboye, D.C. Onwudiwe, Mineralization of antibiotics in wastewater via photocatalysis, Water Air Soil Pollut., 232 (2021) 219.
[9] G. Yashni, A. Al-Gheethi, R. Mohamed, M. Al-Sahari, Reusability performance of green zinc oxide nanoparticles for photocatalysis of bathroom greywater, Water Pract. Technol., 16 (2021) 364–376.
[10] A. Fraiese, V. Naddeo, C.S. Demirel, M. Prado, A. Cesaro, T. Zarra, H. Liu, V. Belgiorno, F. Ballesteros Jr., Removal of emerging contaminants in wastewater by sonolysis, photocatalysis and ozonation, Global Nest J., 21 (2019) 98–105.
[11] M. Khodadadi, T.J. Al-Musawi, H. Kamani, M.F. Silva, A.H. Panahi, The practical utility of the synthesis $FeNi_3$@ SiO_2@TiO_2 magnetic nanoparticles as an efficient photocatalyst for the humic acid degradation, Chemosphere, 239 (2020) 124723, doi: 10.1016/j.chemosphere.2019.124723.
[12] C. Yang, H. Xie, Z. Wang, Y. Tan, N. Wang, Electro-Fenton degradation of high concentration Rhodamine B on nickel foam cathode catalyzed by cucumber bio-templated Fe_3O_4@ PTFE, Int. J. Electrochem. Sci., 16 (2021) 151058, doi: doi: 10.20964/2021.01.54.
[13] K. Meiramkulova, M. Zhumagulov, G. Saspugayeva, Z. Jakupova, M. Mussimkhan, Treatment of poultry slaughter-house wastewater with combined system, Potravinarstvo, 13 (2019) 706–712.
[14] N. Vela, M. Calín, M.J. Yáñez-Gascón, A. el Aatik, I. Garrido, G. Pérez-Lucas, J. Fenoll, S. Navarro, Removal of pesticides with endocrine disruptor activity in wastewater effluent by solar heterogeneous photocatalysis using ZnO/$Na_2S_2O_8$, Water Air Soil Pollut., 230 (2019) 134, doi: 10.1007/s11270-019-4185-y.
[15] M. Antonopoulou, C. Kosma, T. Albanis, I. Konstantinou, An overview of homogeneous and heterogeneous photo-catalysis applications for the removal of pharmaceutical compounds from real or synthetic hospital wastewaters under lab or pilot scale, Sci. Total Environ., 765 (2021) 144163, doi: 10.1016/j.scitotenv.2020.144163.
[16] S.A. Asli, M. Taghizadeh, Sonophotocatalytic degradation of pollutants by ZnO-based catalysts: a review, ChemistrySelect, 5 (2020) 13720–13731.
[17] F. Khitab, J. Shah, M.R. Jan, Systematic assessment of visible light driven photocatalysts for the removal of cefixime in aqueous solution sonophotocatalytically, J. Environ. Anal. Chem., (2022), doi: 10.1080/03067319.2022.2025790.
[18] Z. Yan, W. Huang, X Jiang, J. Gao, Y. Hu, H. Zhang, Q. Shi, Hollow structured black TiO_2 with thickness-controllable microporous shells for enhanced visible-light-driven photocatalysis, Microporous Mesoporous Mater., 323 (2021) 111228, doi: 10.1016/j.micromeso.2021.111228.
[19] D. Alrousan, A. Afkhami, K. Bani-Melhem, P. Dunlop, Organic degradation potential of real greywater using TiO_2-based advanced oxidation processes, Water, 12 (2020) 2811, doi: 10.3390/w12102811.
[20] E.M. de la Fournière, J.M. Meichtry, E.A. Gautier, A.G. Leyva, M.I. Litter, Treatment of ethylmercury chloride by heterogeneous photocatalysis with TiO_2, J. Photochem. Photobiol., A, 411 (2021) 113205, doi: 10.1016/j.jphotochem.2021.113205.
[21] C. Alvarado-Camacho, C.O. Castillo-Araiza, R.S. Ruiz-Martínez, Degradation of Rhodamine B in water alone or as part of a mixture by advanced oxidation processes, 209 (2022) 69–82.
[22] S.N. Ahmed, W. Haider, Heterogeneous photocatalysis and its potential applications in water and wastewater treatment: a review, Nanotechnology, 29 (2018) 342001, doi: 10.1088/1361–6528/aac6ea.
[23] M. Samanta, M. Mukherjee, U.K. Ghorai, C. Bose, K.K. Chatto-padhyay, Room temperature processed copper phthalocyanine nanorods: a potential sonophotocatalyst for textile dye removal, Mater. Res. Bull., 123 (2020) 110725, doi: 10.1016/j.materresbull.2019.110725.
[24] A. Al-Bsoul, M. Al-Shannag, M. Tawalbeh, A.A. Al-Taani, W.K. Lafi, A. Al-Othman, M. Alsheyab, Optimal conditions for olive mill wastewater treatment using ultrasound and advanced oxidation processes, Sci. Total Environ., 700 (2020) 134576, doi: 10.1016/j.scitotenv.2019.134576.
[25] V.K. Mahajan, G.H. Sonwane, Effective degradation and mineralization of real textile effluent by sonolysis, photocatalysis, and sonophotocatalysis using ZnO nanocatalyst, Nanochem. Res., 1 (2016) 258–263.
[26] P. Sravandas, L.K. Alexander, Facile hydrothermal synthesis and sonophotocatalytic performance of novel Bi_2WO_6 structure on the degradation of Rhodamine B, Mater. Today: Proc., 46 (2021) 2925–2929.
[27] M. Pirsaheb, N. Moradi, A systematic review of the sonophotocatalytic process for the decolorization of dyes in aqueous solution: synergistic mechanisms, degradation pathways, and process optimization, J. Water Process Eng., 44 (2021) 102314, doi: 10.1016/j.jwpe.2021.102314.
[28] T.J. Al-Musawi, G. McKay, P. Rajiv, N. Mengelizadeh, D. Balarak, Efficient sonophotocatalytic degradation of Acid Blue 113 dye using a hybrid nanocomposite of $CoFe_2O_4$ nanoparticles loaded on multi-walled carbon nanotubes, J. Photochem. Photobiol., A, 424 (2021) 113617, doi: 10.1016/j.jphotochem.2021.113617.
[29] H. Wei, M.H. Rahaman, J. Zhao, D. Li, J. Zhai, Hydrogen peroxide enhanced sonophotocatalytic degradation of Acid Orange 7 in aqueous solution: optimization by Box–Behnken design, J. Chem. Technol. Biotechnol., 96 (2021) 2647–2658.
[30] M.H. Abdurahman, A.Z. Abdullah, N.F. Shoparwe, A comprehensive review on sonocatalytic, photocatalytic, and sonophotocatalytic processes for the degradation of antibiotics in water: synergistic mechanism and degradation pathway, Chem. Eng. J., 413 (2021) 127412, doi: 10.1016/j.cej.2020.127412.
[31] S. Anandan, V.K. Ponnusamy, M. Ashokkumar, A review on hybrid techniques for the degradation of organic pollutants in aqueous environment, Ultrason. Sonochem., 67 (2020) 105130, doi: 10.1016/j.ultsonch.2020.105130.
[32] P. Sathishkumar, R.V. Mangalaraja, O. Rozas, C. Vergara, H.D. Mansilla, M.A. Gracia-Pinilla, S. Anandan, Sonophotocatalytic mineralization of norflurazon in aqueous environment, Chemosphere, 146 (2016) 216–225.
[33] I. Gulkaya, G.A. Surucu, F.B. Dilek, Importance of H_2O_2/Fe^{2+} ratio in Fenton's treatment of a carpet dyeing wastewater, J. Hazard. Mater., 136 (2006) 763–769.
[34] P. Kumar, T.T. Teng, S. Chand, K.L. Wasewar, Fenton oxidation of carpet dyeing wastewater for removal of COD and color, Desal. Water Treat., 28 (2011) 260–264.
[35] R. Poblete, E. Cortes, G. Salihoglu, N.K. Salihoglu, Ultrasound and heterogeneous photocatalysis for the treatment of vinasse from pisco production, Ultrason. Sonochem., 61 (2020) 104825, doi: 10.1016/j.ultsonch.2019.104825.
[36] R.D.C. Soltani, S. Jorfi, M. Safari, M.-S. Rajaei, Enhanced sonocatalysis of textile wastewater using bentonite-supported ZnO nanoparticles: response surface methodological approach, J. Environ. Manage., 179 (2016) 47–57.
[37] G. Asgari, J. Feradmal, A. Poormohammadi, M. Sadrnour-mohamadi, S. Akbari, Taguchi optimization for the removal of high concentrations of phenol from saline wastewater using electro-Fenton process, Desal. Water Treat., 57 (2016) 27331–27338.
[38] APHA, Standard Methods for the Examination of Water and Wastewater, American Public Health Association (APHA), Washington, DC, USA, 2005.

[39] I. Talinli, G.K. Anderson, Interference of hydrogen peroxide on the standard COD test, Water Res., 26 (1992) 107–110.
[40] Z.B. Gönder, G. Balcıoğlu, Y. Kaya, I. Vergili, Treatment of carwash wastewater by electrocoagulation using Ti electrode: optimization of the operating parameters, Int. J. Environ. Sci. Technol., 16 (2019) 8041–8052.
[41] G. Taguchi, Introduction to Quality Engineering—Designing Quality into Products and Processes, Kraus International, Asian Productivity Organization, Japan, 1986.
[42] Y. Kaya, Z.B. Gönder, I. Vergili, A. Ongen, Application of experimental design method for advanced treatment of dairy wastewater by ozonation, Environ. Prog., 38 (2019) 1–9.
[43] M. Kamalia, M. Khalaj, M.E.V. Costac, I. Capela, Optimization of kraft black liquor treatment using ultrasonically synthesized mesoporous tenorite nanomaterials assisted by Taguchi design, Chem. Eng. Sci., 401 (2020) 126040, doi: 10.1016/j.cej.2020.126040.
[44] Y.Ş. Yildiz, E. Şenyiğit, Ş. İrdemez, Optimization of specific energy consumption for Bomaplex Red CR-L dye removal from aqueous solution by electrocoagulation using Taguchi-neural method, Neural Comput. Appl., 23 (2013) 1061–1069.
[45] F. Ozyonar, Optimization of operational parameters of electrocoagulation process for real textile wastewater treatment using Taguchi experimental design method, Desal. Water Treat., 57 (2016) 2389–2399.
[46] Ş. İrdemez, Y.Ş. Yildiz, V. Tosunoğlu, Optimization of phosphate removal from wastewater by electrocoagulation with aluminum plate electrodes, Sep. Purif. Technol., 52 (2006) 394–401.
[47] V.B.K. Mullapudi, A. Salveru, A.J. Kora, An in-house UV-photolysis setup for the rapid degradation of both cationic and anionic dyes in dynamic mode through UV/H_2O_2-based advanced oxidation process, Int. J. Environ. Anal. Chem., (2020) 1–17, doi: 10.1080/03067319.2020.1800002.
[48] S. Sunasee, K.T. Wong, G. Lee, S. Pichiah, S. Ibrahim, C. Park, N.C. Kim, Y. Yoon, M. Jang, Titanium dioxide-based sonophotocatalytic mineralization of Bisphenol A and its intermediates, Environ. Sci. Pollut. Res., 24 (2017) 15488–15499.
[49] B. Kakavandi, M. Ahmadi, Efficient treatment of saline recalcitrant petrochemical wastewater using heterogeneous UV-assisted sono-Fenton process, Ultrason. Sonochem., 56 (2019) 25–36.
[50] M. Tir, N. Moulai-Mostefa, M. Nedjhioui, Optimizing decolorization of methylene blue dye by electrocoagulation using Taguchi approach, Desal. Water Treat., 55 (2015) 2705–2710.
[51] R.N. Padovan, E.B. Azevedo, Combining a sequencing batch reactor with heterogeneous photocatalysis (TiO_2/UV) for treating a pencil manufacturer's wastewater, Braz. J. Chem. Eng., 32 (2015) 99–106.
[52] S.D. Ayarea, P.R. Gogate, Sonocatalytic treatment of phosphonate containing industrial wastewater intensified using combined oxidation approaches, Ultrason. Sonochem., 51 (2019) 69–76.
[53] A.V. Karim, A. Shriwastav, Degradation of ciprofloxacin using photo, sono, and sonophotocatalytic oxidation with visible light and low-frequency ultrasound: degradation kinetics and pathways, Chem. Eng. J., 392 (2020) 124853, doi: 10.1016/j.cej.2020.124853.
[54] E. Hapeshi, Io. Fotiou, D. Fatta-Kassinos, Sonophotocatalytic treatment of ofloxacin in secondary treated effluent and elucidation of its transformation products, Chem. Eng. J., 224 (2013) 96–105.
[55] S.G. Poulopoulos, G. Ulykbanova, C.J. Philippopoulos, Photochemical mineralization of amoxicillin medicinal product by means of UV, hydrogen peroxide, titanium dioxide and iron, Environ. Technol., 42 (2019) 2941–2949.
[56] S.D. Ayarea, P.R. Gogate, Sonophotocatalytic oxidation based treatment of phthalocyanine pigment containing industrial wastewater intensified using oxidising agents, Sep. Purif. Technol., 233 (2020) 115979, doi: 10.1016/j.seppur.2019.115979.
[57] S.G. Poulopoulos, G. Ulykbanova, C.J. Philippopoulos, Photochemical mineralization of amoxicillin medicinal product by means of UV, hydrogen peroxide, titanium dioxide and iron, Environ. Technol., 42 (2021) 2941–2949.
[58] D. Kanakaraju, C.A. Motti, B.D. Glass, M. Oelgemoller, Photolysis and TiO_2-catalysed degradation of diclofenac in surface and drinking water using circulating batch photoreactors, Environ. Chem., 11 (2014) 51–62.
[59] G. Dogdu Okcu, T. Tunacan, E. Dikmen, Photocatalytic degradation of yellow 2G dye using titanium dioxide/ultraviolet A light through a Box–Behnken experimental design: optimization and kinetic study, J. Environ. Sci. Health A, 54 (2019) 136–145.
[60] G.K. Dinesh, S. Anandan, T. Sivasankar, Synthesis of Fe-doped Bi_2O_3 nanocatalyst and its sonophotocatalytic activity on synthetic dye and real textile wastewater, Environ. Sci. Pollut. Res., 23 (2016) 20100–20110.
[61] F. Ghanbari, A. Yaghoot-Nezhad, S. Wacławek, K.-Y.A. Lin, J. Rodríguez-Chueca, F. Mehdipour, Comparative investigation of acetaminophen degradation in aqueous solution by UV/chlorine and UV/H_2O_2 processes: kinetics and toxicity assessment, process feasibility and products identification, Chemosphere, 285 (2021) 131455, doi: 10.1016/j.chemosphere.2021.131455.
[62] E.S. Elmolla, M. Chaudhuri, The feasibility of using combined TiO_2 photocatalysis-SBR process for antibiotic wastewater treatment, Desalination, 272 (2011) 218–224.
[63] T. Steven, R. Nawaz, N.T. Sahrin, K.M. Lee, C.L. Bianchi, C.F. Kait, H_2O_2-assisted sonophotocatalytic degradation of diclofenac using a visible light-active flower-like micron-sized TiO_2 photocatalyst, Malays. J. Chem., 23 (2021) 108–125.
[64] T.A. Bullo, Y.M. Bayisa, M.S. Bultum, Optimization and biosynthesis of calcined chicken eggshell doped titanium dioxide photocatalyst based nanoparticles for wastewater treatment, SN Appl. Sci., 4 (2022) 17, doi: 10.1007/s42452-021-04900-1.
[65] R.D.C. Soltani, M. Safari, Periodate-assisted pulsed sonocatalysis of real textile wastewater in the presence of MgO nanoparticles: response surface methodological optimization, Ultrason. Sonochem., 32 (2016) 181–190.
[66] Y.Ş. Yildiz, Optimization of Bomaplex Red CR-L dye removal from aqueous solution by electrocoagulation using aluminum electrodes, J. Hazard. Mater., 153 (2008) 194–200.
[67] Z.I. Abbas, A.S. Abbas, Optimization of the electro-Fenton process for COD reduction from refinery wastewater, Environ. Eng. Manage., 19 (2020) 2029–2037.
[68] E. Nas, N. Altan Özbek, Optimization the machining parameters in turning of hardened hot work tool steel using cryogenically treated tools, Surf. Rev. Lett., 27 (2020) 1950177, doi: 10.1142/S0218625X19501774.
[69] P.H. Sreeja, K.J. Sosamony, A comparative study of homogeneous and heterogeneous photo-Fenton process for textile wastewater treatment, Proc. Technol., 24 (2016) 217–223.
[70] M.S. Phadke, Quality Engineering Using Robust Design, Prentice Hall, New Jersey, 1989, pp. 61–292.
[71] Ö. Gökkuş, F. Çoşkun, M. Kocaoğlu, Y.Ş. Yıldız, Determination of optimum conditions for color and COD removal of Reactive Blue 19 by Fenton oxidation process, Desal. Water Treat., 52 (2014) 6156–6165.
[72] M. Yilmaz, M.E. Keskin, Optimal okuma şartlarının Taguchi yöntemiyle belirlenmesi, Acad. Platform J. Eng. Sci., 7 (2019) 25–32.
[73] R. Khalegh, F. Qaderi, Optimization of the effect of nanoparticle morphologies on the cost of dye wastewater treatment via ultrasonic/photocatalytic hybrid process, Appl. Nanosci., 9 (2019) 1869–1889.